Hindawi
Journal of Nanomaterials
Volume 2018, Article ID 8987348, 7 pages
https://doi.org/10.1155/2018/8987348

Research Article

Synthesis of Fluorescent Polythiophene Dots

Zhen Liu,[1] Alaa Nahhas,[2] Li Liu,[3] Earl Ada,[2] Xinyu Zhang,[1] and Sanjeev K. Manohar[2]

[1]*Department of Chemical Engineering, Auburn University, Auburn, AL 36849, USA*
[2]*Department of Chemical Engineering, University of Massachusetts Lowell, Lowell, MA 01854, USA*
[3]*Department of Radiology, University of Texas Southwestern Medical Center, Dallas, TX 75390, USA*

Correspondence should be addressed to Xinyu Zhang; xzz0004@auburn.edu and Sanjeev K. Manohar; sanjeev_manohar@uml.edu

Received 20 July 2017; Accepted 9 May 2018; Published 16 August 2018

Academic Editor: Oscar Perales-Pérez

Ring-functionalized semiconducting polythiophene dots (Pdots) were synthesized rapidly and in one step by the hydrazine hydrate reduction of doped parent polythiophene, obtained by conventional chemical oxidation of thiophene monomer by $FeCl_3$ in anhydrous acetonitrile. Dispersions of these Pdots display robust (pseudo) solvatochromism and solvatofluorism. Polythiophene Pdots exhibit significant cytotoxicity towards prostate cancer cells (expected) although when injected subcutaneously *in vivo* in live mouse, no toxicity is observed for 24 days when monitored in real time using fluorescence imaging.

1. Introduction

In contrast to the wide technological use of conducting polymers in electronic and optoelectronic devices, their application in biomedicine (particularly *in vivo*) has been limited due to dopant leaching and attendant conductivity issues at physiological pH. It is only fairly recently that conducting polymers have made a genuine transition into biomedicine as semiconducting polymer dots (Pdots), where the strong fluorescence exhibited in their undoped electrically insulating state is used to advantage [1–4]. A combination of high intrinsic absorptivity of conjugated polymers and densely packed nanoscale morphology confers Pdots with high chromophore density and very high brightness [5]. Their all-organic nature also often leads to biocompatibility and low toxicity [6].

In this study, we show that semiconducting parent polythiophene Pdots are readily synthesized and can be used as versatile bioimaging agents. Unlike ring-substituted polythiophene, the parent system stands somewhat alone among conducting polymers where its insolubility, intractability, and infusibility severely limits its use [7]. We have described a workaround where thin films of nanofibrillar doped parent polythiophene deposit directly on inert substrates during a chemical oxidative polymerization of thiophene by in situ adsorption polymerization, thereby bypassing all postsynthesis processing steps [8]. We now show that the doped polythiophene powder obtained during the synthesis, when treated with hydrazine hydrate, yields undoped ring-functionalized (Cl, OH) polythiophene powder that disperses in a variety of organic solvents as 10–25 nm diameter Pdots that are highly fluorescent.

2. Experimental Section

In a typical synthesis of polythiophene Pdots (Scheme 1), a solution of 10 ml of 1.0 M anhydrous $FeCl_3$ in anhydrous acetonitrile is added via syringe to a magnetically stirred solution of thiophene monomer (1 ml, 12.5 mmol) in anhydrous acetonitrile (60 ml) in a flask that is continuously purged with nitrogen. The mixture turns dark immediately upon addition of $FeCl_3$, and after 2 h, the resulting black precipitate is suction filtered and washed with copious amounts of acetonitrile. Vacuum drying in an oven at 80°C for 12 h yields ~250 mg of doped polythiophene exhibiting a room temperature conductivity of ~3 S/cm (4-probe, pressed pellet). About 100 mg of freshly synthesized doped polythiophene is then dispersed (magnetically stirred) in a beaker containing ethanol (100 ml), and hydrazine hydrate (2 ml, 40 mmol) is added all at once. Over a period of 12 h, the precipitate changes color from black to red that is consistent with a conversion to undoped polythiophene.

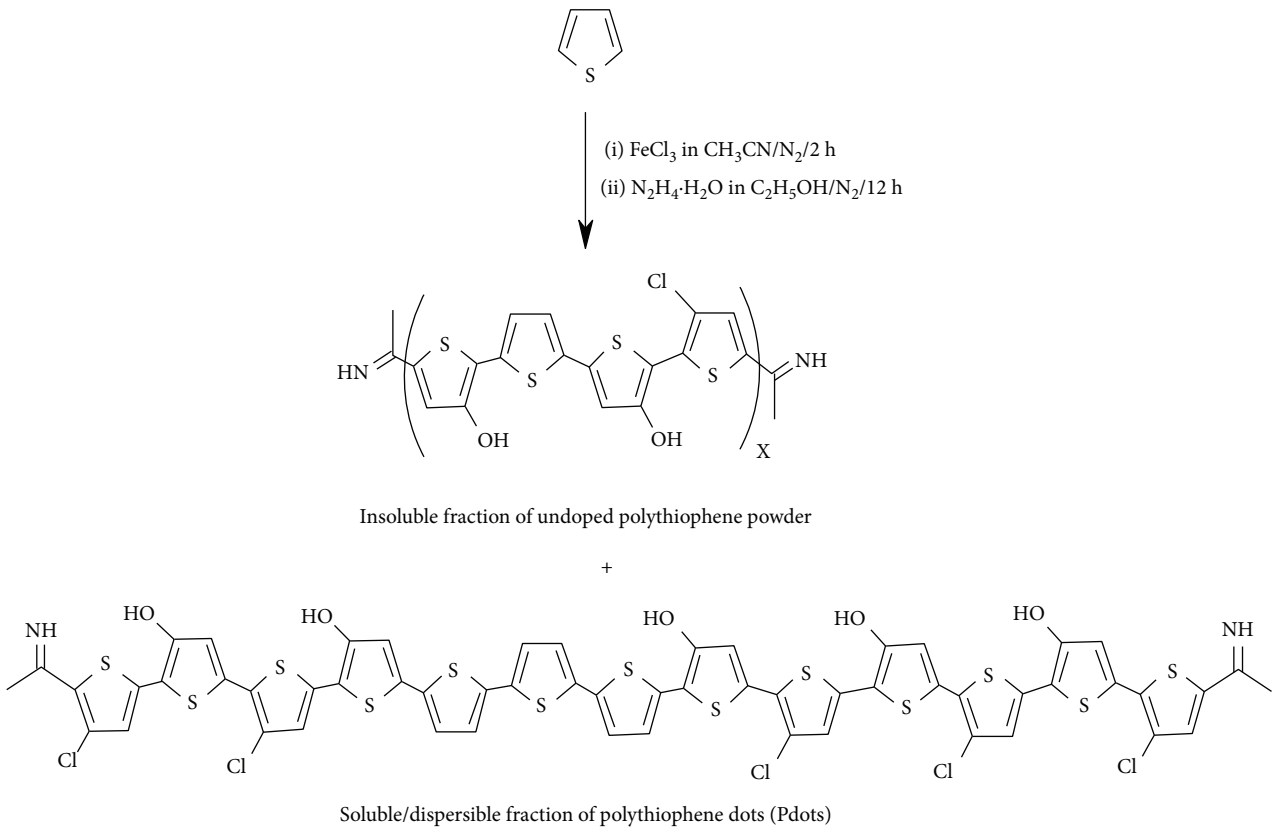

Scheme 1: Chemical synthesis of fluorescent polythiophene Pdots.

3. Results and Discussion

3.1. Characterization of Polythiophene Pdots. Elemental analysis of the red-brown powder obtained after hydrazine hydrate treatment, C: 39.82, H: 1.68, N: 2.11, S: 25.42, O: 11.84, and Cl: 6.62, total: 87.49 (ash residue), is consistent with a polythiophene backbone structure with a C/S ratio of 1.57 (theoretical C/S = 1.50) containing a significant amount of chlorine and oxygen functional groups. X-ray photoelectron spectroscopy indicates that oxygen is present predominantly as OH (along with some C=O) (SI).

This hydrazine hydrate-reduced polythiophene powder disperses readily in water containing 3% polysorbate surfactant (Tween-80) as Pdots with average diameter of ~45 nm. The particle size can be lowered further (to ~14 nm) when it is precipitated from a solution in N-methyl-2-pyrrolidone (NMP). Transmission electron microscopy (TEM) images of Pdots obtained from aqueous dispersions show that while there are some larger-size particles (~45 nm), most of the Pdots cluster around ~14 nm (Figure 1, SI) [9, 10]. Dynamic light-scattering data also show an average particle size of 14 nm. Analytical, spectroscopic, and particle size data are consistent across multiple synthetic batches showing that while the product composition might be complex as one might expect from an as-synthesized product, the simple two-step oxidation-reduction synthesis route yields polythiophene Pdots having reliable and reproducible physical and chemical properties.

Freshly synthesized undoped polythiophene powder is also sparingly soluble in various organic solvents, such as diethyl ether, methanol, tetrahydrofuran (THF), dimethylsulfoxide (DMSO), dimethylformamide (DMF), and NMP. For example, ~23% of the polymer dissolves in NMP while ~5% dissolves in tetrahydrofuran (THF). Solutions of Pdots in organic solvents display unusual properties. For instance, there is no "streaking" in a thin-layer chromatography (TLC) plate as one would expect from a complex polymeric mixture. The polymer spotted on a TLC plate moves as a single spot in solvent mixtures of DMSO and hexane very much like a pure compound. In contrast, MALDI/TOF indicates a complex mixture (SI). Importantly, ^{1}H NMR in DMSO d_6 shows large anomalous upfield peaks (~0 ppm) that are inconsistent with the elemental composition. It is tempting to suggest that these are highly solvated dispersions that happen to display typical solution properties.

For example, solutions of Pdot in organic solvents display marked solvatochromic shifts that are similar in magnitude to what is observed in substituted polythiophenes. The electronic absorption peak (λ_{max}) shifts from 350 nm in diethyl ether to 460 nm in NMP (Figure 2(a)). Typically, solvatochromic shifts in polythiophene derivatives have been attributed to charge transfer between the polymer and various solvents [11] and/or to a different polymer conformation in solution [12, 13]. In contrast, in our Pdot solutions where chains are very tightly packed (almost dispersions), one cannot readily extend these rationalizations to account for

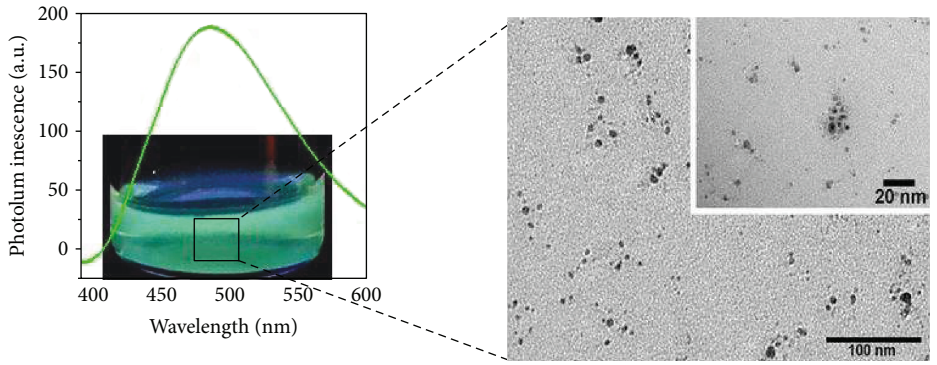

Figure 1: Transmission electron microscopy (TEM) image of polythiophene Pdot dispersion in water containing 3% polysorbate surfactant (Tween-80) obtained by diluting a DMSO solution of polythiophene in excess water and optical image of dispersion and plot of PL intensity versus wavelength showing emission maxima at 485 nm (excitation 365 nm).

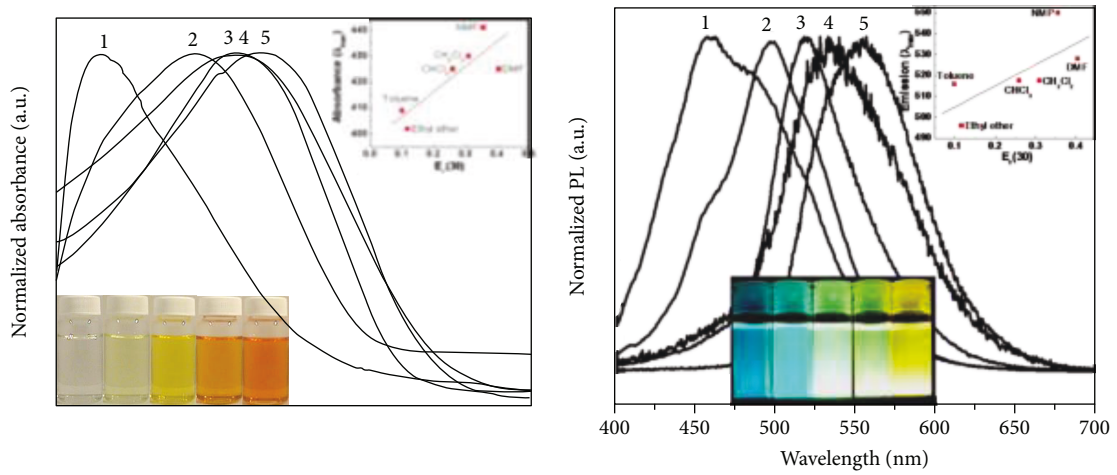

Figure 2: (a) Normalized electronic absorption spectra of Pdots in (1) methanol, (2) ethyl ether, (3) chloroform, (4) DMF, and (5) NMP. Pictures of 1–5 from left to right. Inset: plot of l_{max} versus $E_T(30)$ numbers (solvent polarity). (b) Corresponding emission spectra (excitation at 365 nm).

what appear to be pseudosolvatochromic shifts. Still, it is possible to look for empirical correlations between changes in λ_{max} in different solvents and known solvent parameters, such as dipole moment and dielectric constant. The solvatochromic shift in λ_{max} of Pdot solutions show a relatively solid correlation with the $E_T(30)$ scale, which is a polarity scale derived from changes in the λ_{max} of the lowest energy charge-transfer peak in the electronic spectrum of a highly aromatic zwitterionic betaine dye, pyridinium-*N*-phenolate betaine, in a given solvent [14, 15].

Importantly, our Pdot dispersions are highly fluorescent and show strong solvatofluoric phenomena (Figure 2(b)). The emission maximum (λ_{max}) shifts from 497 nm in diethyl ether to 555 nm in NMP. Once again, there is a definite but somewhat weaker correlation between emission maxima (λ_{max}) in different solvents with the $E_T(30)$ polarity scale that is to be contrasted with the very weak correlation with other solvent polarity scales. Again, it is important to point out that only a small fraction of the polythiophene powder is "soluble" in organic solvents. Since different solvents have different amounts of Pdot, one cannot readily rationalize solvatochromic and solvatofluoric shifts in λ_{max} with the $E_T(30)$ scale. The intense fluorescence observed, however, opens new opportunities for use as bioimaging agents [3].

The relative quantum yield (QY) versus fluorescein was calculated using the equation $Q_S = Q_R(I_S/I_R)(A_R/A_S)(\eta_S/\eta_R)$ [16]where Q_S, I_S, A_s, and η_s are the QY, area under the curve, absorbance intensity, and refractive index values, respectively, for Pdots in NMP and Q_r, I_r, A_r, and η_r are the corresponding values for fluorescein in water. A relative QY value of 72.7% was obtained for Pdots at an excitation wavelength of 460 nm (λ_{max} of Pdot in NMP) using values of 0.91, 1.33, and 1.47 for Q_r, η_r, and η_s, respectively (SI).

The aqueous Tween-80-supported Pdot dispersion is also highly fluorescent with an emission peak at 485 nm (excitation at 365 nm) with a full width at half maxima (FWHM) value of 110.9 nm. For instance, luminescent organic dyes and QDs display FWHM values typically in the 50–100 nm range.

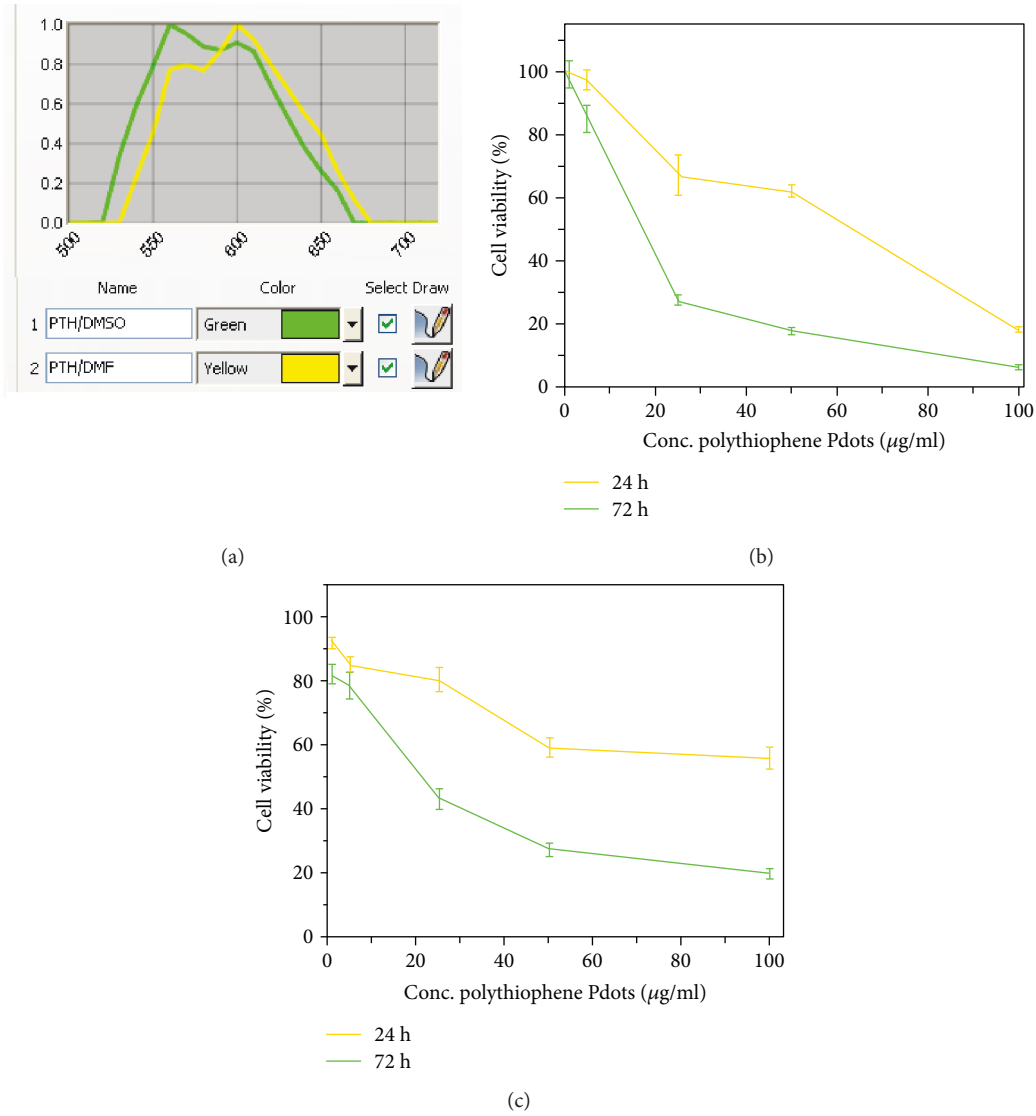

Figure 3: *In vitro* evaluation of cytotoxicity of polythiophene Pdots in prostate cancer PC3 cells: (a) wavelength and fluorescent imaging for Pdots from DMF (right) and DMSO (left) (inset); cytotoxicity at 24 h and 72 h of Pdots (b) from DMF and (c) from DMSO. Excitation wavelength: 455 nm (blue filter) and 560 nm (green filter).

3.2. Bioimaging. Fluorescent materials for biosensing and bioimaging include metal ions [17], conjugated polyelectrolytes [18], functionalized nanoparticles (NPs) involving quantum dots (QDs) [19–22], magnetic particles (MPs) [23, 24], noble metal NPs [25–28], functionalized proteins [29–31], carbon dots [32, 33], and, more recently, conjugated polymers. The effect of polythiophene Pdots on prostate cancer cell PC3 viability was determined by crystal violet assay. Pdots of different concentrations (1, 5, 25, 50, and 100 μg/ml) were tested on human prostate cancer cells by diluting solutions in DMSO or DMF. The final concentration of DMSO was <0.5%. Expectedly, the plot of Pdot concentration versus relative viable cells (Figure 3) shows that it is very cytotoxic to human prostate cancer cells (PC3) with cytotoxicity increasing after 24 h.

For *in vivo* studies, this concentration was halved, that is, diluted further to 12.5 μg/ml. Based on the cytotoxicity data above and looking at the chemical composition with a significant amount of Cl groups, we anticipated polythiophene Pdots to display even greater toxicity *in vivo*.

Surprisingly, polythiophene Pdots show very low cytotoxicity *in vivo* (Figure 4). For example, Pdots were injected subcutaneously *in vivo* in a live mouse and its photostability [34, 35] and cytotoxicity [36] were probed relative to classically applied NPs, MPs, and QDs. For *in vivo* fluorescent imaging experiments, 20 μl of a Pdot dispersion in water (12.5 μg/ml) was injected subcutaneously into two spots of the flank of C57BL/6mice. Mice were anesthetized using a mixture of ketamine, xylazine, and acepromazine, and then fluorescent images were acquired *in vivo* by in situ monitoring at 10 min, 30 min, 60 min, and 24 h after injection. For clearance studies, fluorescent images were acquired with several day intervals during a 24-day period. To further understand the temporal effects of cytotoxicity,

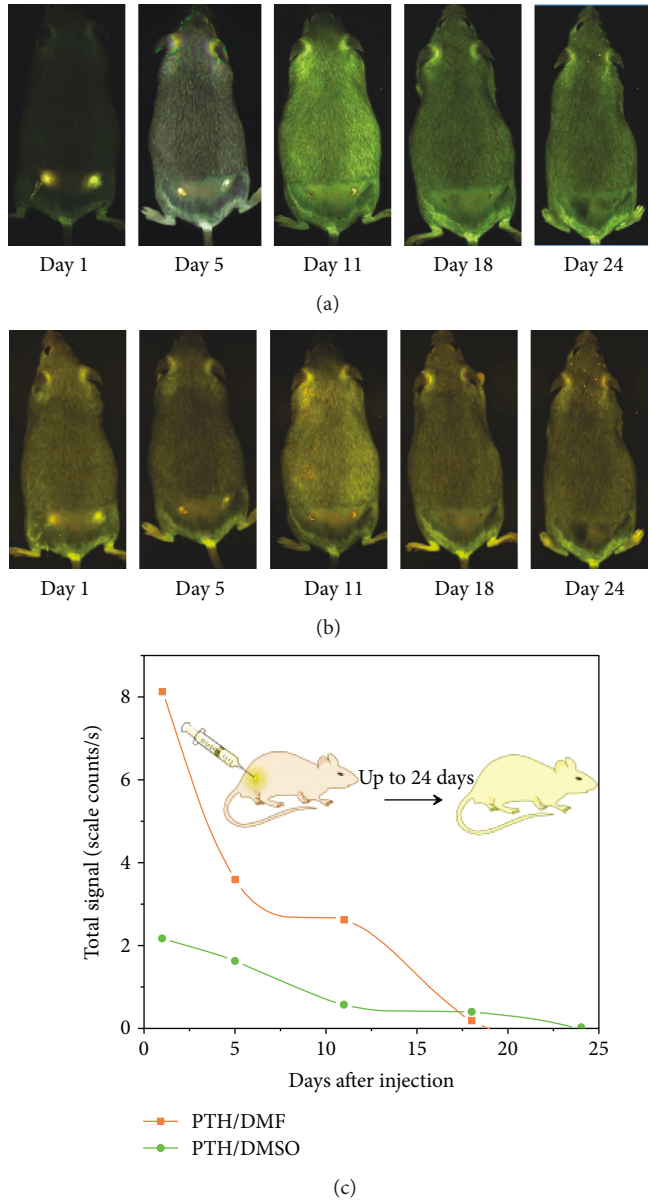

FIGURE 4: *In vivo* imaging of changes in fluorescence intensity of Pdots subcutaneously injected in two spots of the flank of C57BL/6mice over a period of 24 days, (a) from DMSO, (b) from DMF, and (c) plot of total signal intensity over a period of 24 days. Excitation wavelength: 455 nm (blue filter) and 560 nm (green filter).

Pdots with fluorescence emission peaks in the blue range were used and imaged using a multispectral CRi Maestro fluorescent imaging system with blue filter and green filter (Figures 4(a) and 4(b)). The fluorescence intensity changes over a 24-day period indicating excellent fluorescence stability [37], slow degradation [38], and low toxicity.

Polythiophene Pdots appear to be toxic to cells but not to live mice. This apparent contradiction between *in vitro* and *in vivo* toxicities can be rationalized on the basis of differences in dosage. A similar discrepancy has been observed in the toxicity of CdSe QDs *in vivo* and *in vitro* studies. Under cell culture conditions, the concentration of Pdots remains high for an extended period of time which induces cytotoxicity, whereas when injected into a live mouse, the concentration is continuously in flux; that is, the site-specific (subcutaneous) dose is not elevated enough to induce toxicity. Compared to QDs, our Pdots are expected to be safer because they are completely excreted over 24 days whereas even QDs that are found to be nontoxic are retained in the liver or spleen [39]. It is important to note, however, that these results are for subcutaneous injection and not intravenous injection, so one has to be careful while making comparisons with existing organic fluorescent imaging probes. Importantly, the emission range is still short of the near-IR range that is typical of developmental bioimaging probes. However, the direct one-step access to ring-functionalized undoped polythiophene opens new opportunities to modify the synthesis to tailor Pdots having these desirable properties including how to target specific organs and/or to reduce clearance time in the body. For example, pegylation of the

polymer backbone during the reduction step (or postsynthesis) is expected to increase hydrophilicity and reduce (renal) clearance times significantly [3]. All this is enabled by facile access to a hydroxyl-functionalized polymer backbone in essentially one step, for example, simultaneous reduction and ring substitution of the polythiophene backbone during the reaction with hydrazine hydrate. By leveraging the reduction reaction, it might be possible to gain access to a large family of luminescent polythiophenes with preselected properties. In this sense, the current study is more about a simple and rapid new synthetic method to Pdots with the imaging data providing early validation for surprisingly low *in vivo* toxicity and overall potential for bioimaging.

4. Conclusions

In summary, this is the first account of solvatochromism and solvatofluorism in polythiophene obtained directly from thiophene monomer and of corresponding Pdots that can be used for *in vivo* imaging. This rediscovery of the technological uses of the parent polythiophene system could lead to new opportunities in biomedicine, such as fluorescent probes for peptides and nanotherapeutics and in other areas such as related to photovoltaics. Importantly, our synthetic route using hydrazine hydrate is simple, inexpensive, and rapid and can be readily extended to other conducting polymers, such as PEDOT and polypyrrole.

Conflicts of Interest

The authors declare that they have no conflicts of interest.

Authors' Contributions

Zhen Liu and Alaa Nahhas contributed equally.

Acknowledgments

The authors gratefully acknowledge financial support from Auburn University, the Robert and Gail Ward Endowed Professorship at the University of Massachusetts Lowell (UML), and the University of Texas Southwestern Medical Center.

Supplementary Materials

Additional information can be found in the Supporting Information section on (i) synthesis of doped and undoped polythiophene; (ii) X-ray photoelectron spectroscopy (XPS) of undoped polythiophene; (iii) transmission electron microscopy (TEM) images of soluble, filtered fractions of undoped polythiophene in DMSO and THF; (iv) Fourier transform infrared spectroscopy of doped polythiophene, as-synthesized undoped polythiophene, and DMSO-insoluble fraction of undoped polythiophene; (v) dynamic light-scattering (DLS) data on aqueous dispersions of undoped polythiophene in water containing 2 wt% Tween-80; (vi) matrix-assisted laser desorption ionization mass spectrometry (MALDI) of the DMSO soluble fraction of undoped polythiophene; (vii) thermogravimetric analysis (TGA) of doped and undoped polythiophene; (viii) details of the cytotoxicity assay; and (ix) details on fluorescence imaging studies on undoped polythiophene in DMSO and DMF. Also included is Table 1 that summarizes the optical properties of dispersions of undoped polythiophene in different solvents. *(Supplementary Materials)*

References

[1] A. L. Antaris, H. Chen, K. Cheng et al., "A small-molecule dye for NIR-II imaging," *Nature Materials*, vol. 15, no. 2, pp. 235–242, 2016.

[2] L. Zhang, W. Du, A. Nautiyal, Z. Liu, and X. Zhang, "Recent progress on nanostructured conducting polymers and composites: synthesis, application and future aspects," *Science China Materials*, vol. 61, no. 3, pp. 303–352, 2018.

[3] O. S. Wolfbeis, "An overview of nanoparticles commonly used in fluorescent bioimaging," *Chemical Society Reviews*, vol. 44, no. 14, pp. 4743–4768, 2015.

[4] C. Wu and D. T. Chiu, "Highly fluorescent semiconducting polymer dots for biology and medicine," *Angewandte Chemie International Edition*, vol. 52, no. 11, pp. 3086–3109, 2013.

[5] P.-O. Morin, T. Bura, B. Sun, S. I. Gorelsky, Y. Li, and M. Leclerc, "Conjugated polymers à la carte from time-controlled direct (hetero)arylation polymerization," *ACS Macro Letters*, vol. 4, no. 1, pp. 21–24, 2015.

[6] P. Howes, M. Green, J. Levitt, K. Suhling, and M. Hughes, "Phospholipid encapsulated semiconducting polymer nanoparticles: their use in cell imaging and protein attachment," *Journal of the American Chemical Society*, vol. 132, no. 11, pp. 3989–3996, 2010.

[7] X. Zhang and S. K. Manohar, "Bulk synthesis of polypyrrole nanofibers by a seeding approach," *Journal of the American Chemical Society*, vol. 126, no. 40, pp. 12714-12715, 2004.

[8] X. Zhang, S. P. Surwade, V. Dua, R. Bouldin, N. Manohar, and S. K. Manohar, "Parent polythiophene nanofibers," *Chemistry Letters*, vol. 37, no. 5, pp. 526-527, 2008.

[9] Y. Rong, J. Yu, X. Zhang et al., "Yellow fluorescent semiconducting polymer dots with high brightness, small size, and narrow emission for biological applications," *ACS Macro Letters*, vol. 3, no. 10, pp. 1051–1054, 2014.

[10] W. Sun, J. Yu, F. Ye, Y. Rong, and D. T. Chiu, "Highly fluorescent semiconducting polymer dots for single-molecule imaging and biosensing," in *Biosensing and Nanomedicine VI*, p. 881205, San Diego, CA, USA, 2013.

[11] A. Bolognesi, A. Giacometti Schieroni, C. Botta et al., "High photoluminescence efficiency in substituted polythiophene aggregates," *Synthetic Metals*, vol. 139, no. 2, pp. 303–310, 2003.

[12] V. C. Gonçalves and D. T. Balogh, "Synthesis and characterization of a dye-functionalized polythiophene with different chromic properties," *European Polymer Journal*, vol. 42, no. 12, pp. 3303–3310, 2006.

[13] P. V. Shibaev, K. Schaumburg, T. Bjornholm, and K. Norgaard, "Conformation of polythiophene derivatives in solution," *Synthetic Metals*, vol. 97, no. 2, pp. 97–104, 1998.

[14] K. Parikh, K. Cattanach, R. Rao, D.-S. Suh, A. Wu, and S. K. Manohar, "Flexible vapour sensors using single walled carbon nanotubes," *Sensors and Actuators B: Chemical*, vol. 113, no. 1, pp. 55–63, 2006.

[15] C. Reichardt, *Solvents and Solvent Effects in Organic Chemistry*, Wiley-VCH, Weinheim, Germany, 2nd edition, 1988.

[16] J. M. Pringle, O. Ngamna, J. Chen, G. G. Wallace, M. Forsyth, and D. R. MacFarlane, "Conducting polymer nanoparticles synthesized in an ionic liquid by chemical polymerisation," *Synthetic Metals*, vol. 156, no. 14-15, pp. 979–983, 2006.

[17] Y. Jeong and J. Yoon, "Recent progress on fluorescent chemosensors for metal ions," *Inorganica Chimica Acta*, vol. 381, pp. 2–14, 2012.

[18] A. Parthasarathy, H. C. Pappas, E. H. Hill, Y. Huang, D. G. Whitten, and K. S. Schanze, "Conjugated polyelectrolytes with imidazolium solubilizing groups. Properties and application to photodynamic inactivation of bacteria," *ACS Applied Materials & Interfaces*, vol. 7, no. 51, pp. 28027–28034, 2015.

[19] S. Carregal-Romero, M. Ochs, and W. J. Parak, "Nanoparticle-functionalized microcapsules for in vitro delivery and sensing," *Nanophotonics*, vol. 1, no. 2, p. 171, 2012.

[20] K.-T. Yong, W.-C. Law, I. Roy et al., "Aqueous phase synthesis of CdTe quantum dots for biophotonics," *Journal of Biophotonics*, vol. 4, no. 1-2, pp. 9–20, 2011.

[21] J. Zhang, D. Wu, M.-F. Li, and J. Feng, "Multifunctional mesoporous silica nanoparticles based on charge-reversal plug-gate nanovalves and acid-decomposable ZnO quantum dots for intracellular drug delivery," *ACS Applied Materials & Interfaces*, vol. 7, no. 48, pp. 26666–26673, 2015.

[22] P. Zrazhevskiy, M. Sena, and X. Gao, "Designing multifunctional quantum dots for bioimaging, detection, and drug delivery," *Chemical Society Reviews*, vol. 39, no. 11, pp. 4326–4354, 2010.

[23] K. Hayashi, K. Ono, H. Suzuki et al., "Electrosprayed synthesis of red-blood-cell-like particles with dual modality for magnetic resonance and fluorescence imaging," *Small*, vol. 6, no. 21, pp. 2384–2391, 2010.

[24] H. Yang, W. Liang, N. He, Y. Deng, and Z. Li, "Chemiluminescent labels released from long spacer arm-functionalized magnetic particles: a novel strategy for ultrasensitive and highly selective detection of pathogen infections," *ACS Applied Materials & Interfaces*, vol. 7, no. 1, pp. 774–781, 2015.

[25] R. R. Arvizo, S. Bhattacharyya, R. A. Kudgus, K. Giri, R. Bhattacharya, and P. Mukherjee, "Intrinsic therapeutic applications of noble metal nanoparticles: past, present and future," *Chemical Society Reviews*, vol. 41, no. 7, pp. 2943–2970, 2012.

[26] S. Bhattacharyya, R. A. Kudgus, R. Bhattacharya, and P. Mukherjee, "Inorganic nanoparticles in cancer therapy," *Pharmaceutical Research*, vol. 28, no. 2, pp. 237–259, 2011.

[27] T. Cochell and A. Manthiram, "Pt@Pd_xCu_y/C core–shell electrocatalysts for oxygen reduction reaction in fuel cells," *Langmuir*, vol. 28, no. 2, pp. 1579–1587, 2012.

[28] M. Liu, L. Zhang, and T. Wang, "Supramolecular chirality in self-assembled systems," *Chemical Reviews*, vol. 115, no. 15, pp. 7304–7397, 2015.

[29] J. O. Keem, I. H. Lee, S. Y. Kim, Y. Jung, and B. H. Chung, "Splitting and self-assembling of far-red fluorescent protein with an engineered beta strand peptide: application for alpha-synuclein imaging in mammalian cells," *Biomaterials*, vol. 32, no. 34, pp. 9051–9058, 2011.

[30] J. L. Toca-Herrera, S. Küpcü, V. Diederichs, G. Moncayo, D. Pum, and U. B. Sleytr, "Fluorescence emission properties of S-layer enhanced green fluorescent fusion protein as a function of temperature, pH conditions, and guanidine hydrochloride concentration," *Biomacromolecules*, vol. 7, no. 12, pp. 3298–3301, 2006.

[31] H. Wang, C. T. Black, and P. Akcora, "Elastic properties of protein functionalized nanoporous polymer films," *Langmuir*, vol. 32, no. 1, pp. 151–158, 2016.

[32] L. Guo, J. Ge, W. Liu et al., "Tunable multicolor carbon dots prepared from well-defined polythiophene derivatives and their emission mechanism," *Nanoscale*, vol. 8, no. 2, pp. 729–734, 2016.

[33] Y. Wang and A. Hu, "Carbon quantum dots: synthesis, properties and applications," *Journal of Materials Chemistry C*, vol. 2, no. 34, p. 6921, 2014.

[34] H. Tang, C. Xing, L. Liu, Q. Yang, and S. Wang, "Synthesis of amphiphilic polythiophene for cell imaging and monitoring the cellular distribution of a cisplatin anticancer drug," *Small*, vol. 7, no. 10, pp. 1464–1470, 2011.

[35] L. Xiong, A. J. Shuhendler, and J. Rao, "Self-luminescing BRET-FRET near-infrared dots for in vivo lymph-node mapping and tumour imaging," *Nature Communications*, vol. 3, no. 1, p. 1193, 2012.

[36] Y. S. Jeong, W. K. Oh, S. Kim, and J. Jang, "Cellular uptake, cytotoxicity, and ROS generation with silica/conducting polymer core/shell nanospheres," *Biomaterials*, vol. 32, no. 29, pp. 7217–7225, 2011.

[37] A. J. Kell, L. Page, S. Tan et al., "The development of a silica nanoparticle-based label-free DNA biosensor," *Nanoscale*, vol. 3, no. 9, pp. 3747–3754, 2011.

[38] S. A. Gevorgyan and F. C. Krebs, "Bulk heterojunctions based on native polythiophene," *Chemistry of Materials*, vol. 20, no. 13, pp. 4386–4390, 2008.

[39] K. M. Tsoi, Q. Dai, B. A. Alman, and W. C. W. Chan, "Are quantum dots toxic? Exploring the discrepancy between cell culture and animal studies," *Accounts of Chemical Research*, vol. 46, no. 3, pp. 662–671, 2013.